Y.-C. Chuang, S. Mordijck, R. Fitzpatrick, R. Reksoatmodjo

SOLPS-ITER simulations to study the impact of aspect ratio on edge fueling neutrals in tokamaks

SOLPS-ITER simulations to study the impact of aspect ratio on edge fueling neutrals in tokamaks

Y.-C. Chuang, S. Mordijck, R. Fitzpatrick, R. Reksoatmodjo

SOLPS-ITER simulations to study the impact of aspect ratio on edge fueling neutrals in tokamaks

Yi-Cheng Chuang[a,*], Saskia Mordijck[a], Richard Fitzpatrick[b] and Richard Reksoatmodjo[c]

[a]*William & Mary, 200 Stadium Dr, Williamsburg, VA 23185, U.S.A.*

[b]*Institute for Fusion Studies, University of Texas at Austin, Austin, TX 78712, U.S.A.*

[c]*Lawrence Livermore National Laboratory, Livermore, CA 94551, U.S.A.*

ARTICLE INFO

ABSTRACT

In this paper, we examine the role of the aspect ratio on the neutral penetration and poloidal distribution for fixed magnetic geometry and plasma profiles using SOLPS-ITER. We start from an H-mode discharge from MAST [9], with its aspect ratio of 1.4 and shift the magnetic equilibrium and vessel in major radius to generate a new SOLPS-ITER simulation, doubling the aspect ratio to 2.8. The neutral density profile perpendicular to the magnetic flux surfaces is fitted by an exponential and we find that the opaqueness defined as the ratio between the electron pedestal density width and the neutral penetration depth is unaffected by changes in the aspect ratio. We do observe an increase in the neutral density close to the X-point on the high field side (HSF) as the aspect ratio increases. This substantial increase on the HFS is linked to an increase in the poloidal particle fluxes which shift down as a function of aspect ratio, leading to an increase in particle flux to the inner divertor and decrease to the outer divertor. The neutral density in the inner divertor is directly proportional to the increase in particle flux.

1. Introduction

The spherical tokamak concept is an attractive concept for a compact magnetic confinement approach to a fusion pilot plant [3]. The pedestal width in a spherical tokamak is wider than in a regular tokamak and recent theoretical simulations indicate that the impact of gyrokinetic instabilities such as Micro Tearing Modes, Tearing modes, and Kinetic Ballooning Modes expand the pedestal width for spherical tokamaks [13]. However, the pedestal pressure structure is a construct of both temperature and density and the impact of ionization on the pedestal density structure is an active topic of research in conventional tokamaks [8, 17, 2, 10]. The impact of aspect ratio on ionization, neutral density profiles has not yet been explored and could influence the design of a pilot plant with respect to fueling and the fuel cycle.

In this paper, we use SOLPS-ITER [1] to investigate whether the aspect ratio affects the neutral density penetration and poloidal distribution of neutrals. Prior work in conventional tokamaks showed that the neutral density and ionization at high opaqueness have limited effect on the pedestal density structure [8, 10]. Opaqueness of neutrals in the pedestal is defined as a dimensionless number by taking the ratio of the pedestal density width, Δn_e to the penetration depth of the neutrals λ_{n0}. The penetration depth is found by fitting an exponential to the neutral density profile calculated in SOLPS-ITER. A heuristic approximation of opaqueness that doesn't depend on these measured and/or modeled quantities is $n_e \times a$, where $n_e = (n_e^{PED} + n_e^{SEP})/2$ and a is the minor radius [10]. Recent results, comparing the penetration and ionization of hydrogen and deuterium at various levels of opaqueness has shown good agreement with the heuristic model [2, 11].

As experimental measurements for neutral densities inside the separatrix are not readily available, we rely on the heuristic approximation to identify lower and higher opaqueness regimes. In conventional tokamaks at low opaqueness, the ionization plays an important role in determining the pedestal density structure. The penetration of neutrals can shift the pedestal density outwards [6]. It also affects the width of the pedestal density [2]. At low opaqueness, changes in divertor closure has a substantial influence on the poloidal distribution of the neutrals, which in turn affects the width of the electron density pedestal [12]. SOLPS-ITER modeling and experiments show that these poloidal asymmetries and changes to the pedestal density structure disappear at higher opaqueness [10, 11].

As the heuristic model depends only on the minor radius, it doesn't encompass the influence of aspect ratio and thus machine size. To isolate the impact of aspect ratio, we use SOLPS-ITER to model an MAST H-mode discharge [9] and match the midplane electron density and temperature profiles. Next we shift the magnetic equilibrium and the vessel as a function of the major radius in multiple steps and create a new grid for the SOLPS-ITER simulations, see section 2. By fitting the SOLPS-ITER simulations we can extract the opaqueness $\eta = \Delta n_e / \lambda_{n0}$ as a function of aspect ratio, which is discussed in section 3. We find that the aspect ratio has no impact on the neutral opaqueness, but a change in the aspect ratio does affect the poloidal neutral density formation. As the aspect ratio increases from 1.4 to 2.8, an increase in the neutral density on the high field side (HFS) is observed, see section 4. We observe that this increase is the result of an increase in the poloidal Scrape-Off Layer particle flux, which depends on R, the major radius.

---

*Corresponding author

✉ ychuang@wm.edu (Y. Chuang)

ORCID(s):

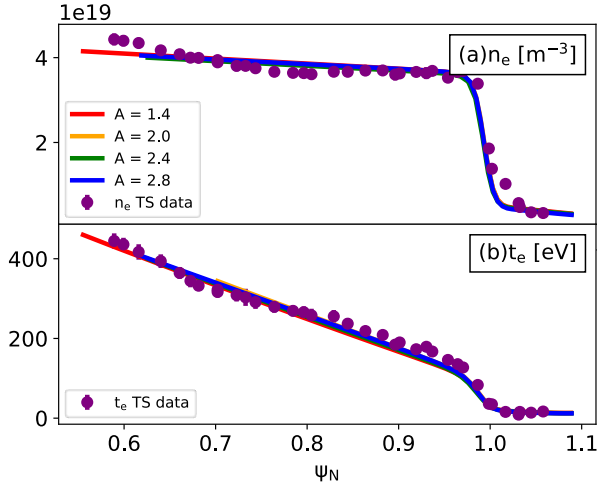## 2. SOLPS-ITER simulations varying aspect ratio

Figure 1: (a) Electron density and (b) temperature mid-plane profile for discharge 27205 at 0.275 s. The purple circles and error bars are from the MAST Thomson Scattering system. The lines are the SOLPS-ITER simulations for the various aspect ratios starting at 1.4 (MAST, red), 2.0 (orange), 2.4 (green), and 2.8 (blue).

The baseline MAST type-I ELM H-mode plasma scenario (27205) in this paper is a lower single null plasma, with a plasma current of 600 kA a toroidal field of 0.55 T and a $q_{95} \sim 2.8$ during the H-mode phase which starts at 0.24 s. The line-averaged density of 4×10^{19} m^{-3} and 3.6 MW of neutral beam injected (NBI) power is injected. The mid-plane profiles of the electron density and temperature are measured with the Thomson Scattering system and taken at 0.275 s.

We use the SOLPS-ITER code [1] to model this MAST scenario. The SOLPS-ITER code consists of two codes, $B2.5$ which solves the Braginskii plasma fluid equations, and $EIRENE$, a Monte-Carlo neutral code. Both are coupled together and evolve the solution until a steady-state solution is found. SOLPS-ITER requires user input for the cross-field transport and the transport coefficients are determined by comparing and adjusting the SOLPS-ITER simulations until the simulations match the experimental measurements for the electron density, n_e and temperature, T_e at the midplane, see figure 1. The transport coefficients are identical for all simulations. In addition, the core boundary conditions are set to a fixed density and temperature. The boundaries at the edge of the B2.5 SOL grid and Private Flux Region (PFR) are determined by flux leakage conditions. The particle flux leakage, $\Gamma_{loss} = \alpha_n C_{(s,e)} n_e$ approximates the radial loss as an advection flux based on the sound speed $C_{(s,e)}$, which is scaled by a parameter α_n, which is set to 10^{-3} in all our simulations. The electron heat flux leakage is similar $\Gamma_{loss} = \alpha_e C_{(s,e)} n_e T_e$ and in this case, α_e is set to 10^{-2} in all simulations. The EIRENE simulation initializes 9×10^5 particles and the boundary conditions are set to be fully

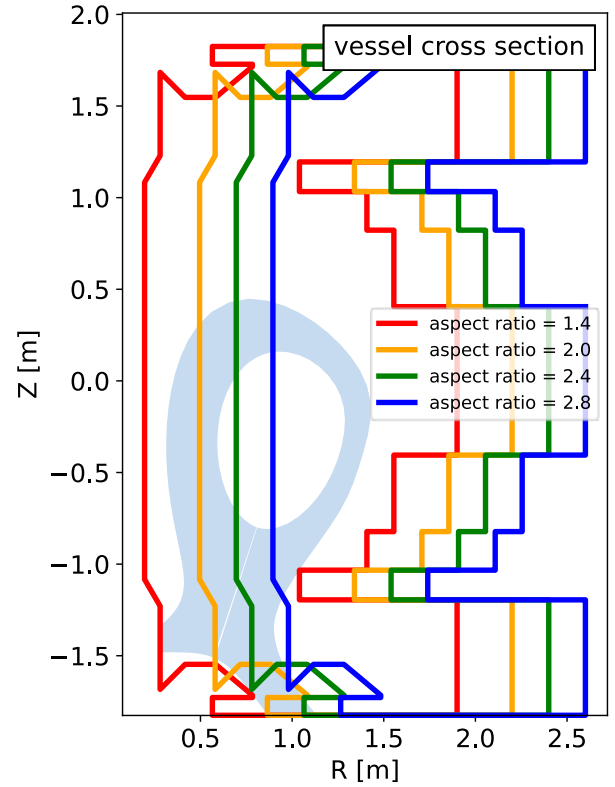recycled, except at the divertor plates, where the recycling is set at 0.99.

Figure 2: Vessel cross-section and magnetic configuration for the SOLPS-ITER simulations for MAST (red). The additional vessel geometries correspond to the shifts in radius and thus aspect ratio at 2.0 (orange), 2.4 (green), 2.8 (blue).

After determining the boundary conditions and transport coefficients based on the MAST experimental data, we shift both the magnetic geometry and the vessel in major radius to regenerate a grid for SOLPS-ITER, see figure 2. The magnetic geometry is shifted along with the vessel structure and provides us with 4 different aspect ratios, 1.4, 2.0, 2.4, and 2.8. In comparison, DIII-D has an aspect ratio of 2.5, and C-Mod and ITER have an aspect ratio of 3.1. With the same boundary conditions and perpendicular transport coefficients, all the simulations have identical electron density and temperature profiles at the midplane, see figure 1. The location of the inner grid boundary depends on the grid reconstruction but is always far enough from the separatrix to allow us to study the impact on the neutral density.

3. Neutral opaqueness

Opaqueness is defined as the ratio of the electron pedestal density width and the neutral penetration length $\eta = \Delta n_e / \lambda_{n0}$. It is a dimensionless number that allows for the comparison between different devices, experimental scenarios, as well as if there is a poloidal dependence due to magnetic flux expansion and difference in neutral sources poloidally.
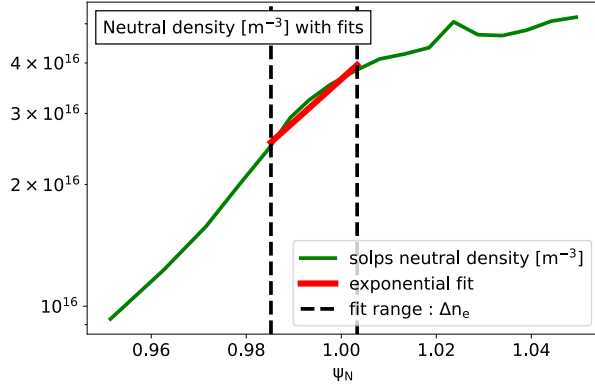
Figure 3: SOLPS-ITER calculated neutral density profile at the midplane (green). The density pedestal width and location are indicated by the dashed black lines. The exponential fit to the profile for the pedestal width region is shown in red.

Figure 4: (a) Electron density pedestal width (Δn_e) (b) neutral penetration length (λ_{n0}), and (c) opaqueness (η) versus poloidal angle for various aspect ratios starting at 1.4 (MAST, red), 2.0 (orange), 2.4 (green), 2.8 (blue). The dashed black vertical lines indicate the location of the lower X-point in the simulation. The brown dashed line is the outer midplane and the gray dashed line is the inner midplane.

To extract the electron density pedestal width, Δn_e we fit a tanh to the SOLPS-ITER modeled electron density profiles [8]. The tanh fit is applied at each poloidal angle of the SOLPS-ITER simulation and mapped for each poloidal location from flux space to machine coordinates. The resulting Δn_e as a function of poloidal angle is shown in figure 4 a). The pedestal width is constant in flux space, as the electron quantities are constant on a flux surface, but due to flux expansion, the pedestal width is not constant in machine coordinates. The Grad-Shafranov shift means that the width is narrower on the LFS and wider on the HFS, by about a factor 2 [19]. The width increases substantially close to the X-point, which due to magnetic geometry flux, leads to a pronounced flux expansion. As all simulations had the same electron density pedestal, no variation in the pedestal density width between simulations, and thus aspect ratio is observed for the pedestal width.

To extract the neutral penetration depth λ_{n0}, we fit an exponential to the neutral density calculated by SOLPS-ITER at each poloidal location [16], see figure 3.

$$n_0 = n_0^{sep} e^{-r/\lambda_{n0}} \tag{1}$$

n_0 is the neutral density, n_0^{sep} is the neutral density at the separatrix and λ_{n0} is the neutral penetration depth and r is the minor radius coordinate at each poloidal location. The neutral penetration depth λ_{n0} is wider than the pedestal width, which has been observed in DIII-D experimentally at low opaqueness [2], especially on the LFS, see figure 4. The neutral penetration depth, λ_{n0}, also increases on the HFS similar to the pedestal width, but only by a factor of 1.5, and again a large increase is observed close to the lower X-point. There is no substantial variation observed between the different aspect ratios, which suggests that with respect to neutral dynamics when plasma conditions are identical, the aspect ratio has little influence on neutral dynamics inside the separatrix.

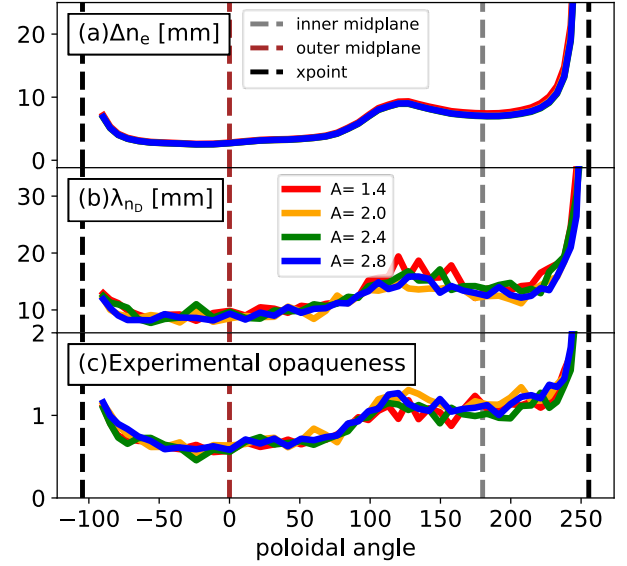With both the pedestal density width and the neutral penetration depth we can now calculate the opaqueness,

$\eta = \Delta n_e / \lambda_{n0}$, see figure 4. The opaqueness is close to 1 as a function of the poloidal angle for all aspect ratios. On the LFS, the opaqueness is just below 1, and on the HFS, the opaqueness increases above 1. The results are very sensitive to small variations in either electron density width as a function of flux expansion. This is best illustrated at the X-point, where counter to intuition we observe an increase in opaqueness, while it is often assumed that X-point fueling dominates. The overall observation is that the opaqueness is unaffected by changes in aspect ratio while keeping all other parameters constant. This implies that any change in opaqueness as a function of aspect ratio will be due to changes in plasma transport and pedestal structure [5, 13].

4. Poloidal variation of neutral density

While the penetration depth might not vary inside the separatrix, this does not mean that the neutral density itself was not affected by changes in aspect ratio. Figure 5 shows the 2D neutral density profiles calculated by SOLPS-ITER for the original MAST case and the case with the large shift in R and an aspect ratio of 2.8. The light colors represent higher neutral densities and the dark colors are lower neutral densities. The neutral densities on the HFS are higher for the shifted case than for the original MAST case.

To identify systemic changes in the neutral density as a function of aspect ratio, we investigate the neutral density at the separatrix as a function of poloidal angle. The neutral density at the separatrix, n_0^{SEP}, as calculated by equation 1 instead of using the direct values from the EIRENE simulation. The use of the fit 'smooths' the noisy variation in
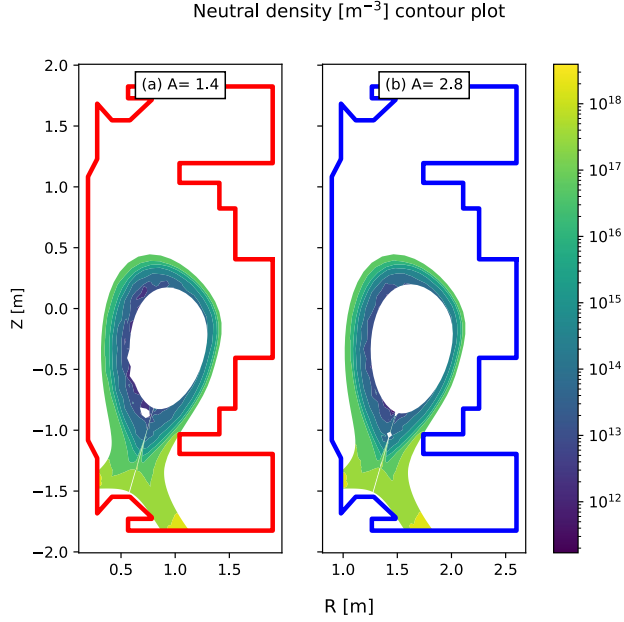
Neutral density [m^{-3}] contour plot

Figure 5: Neutral density contour plot calculated with SOLPS-ITER for aspect ratio (a) 1.4 (left, MAST) and (b) 2.8 (right).
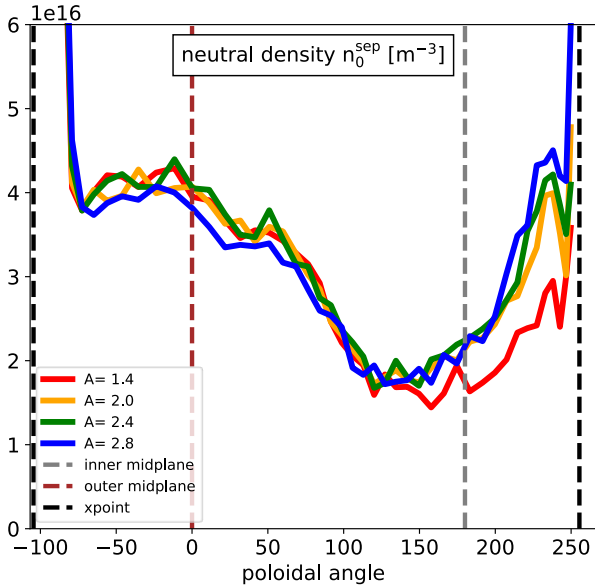

Figure 6: Fitted neutral density. The data colors and vertical dash lines have the same label as in figure 4.

neutral density that occurs as a result of Monte-Carlo noise and simplifies the comparison. Figure 6 shows the separatrix neutral densities as a function of poloidal angle, with the LFS midplane at 0 degrees and the HFS midplane at 180. The dark dashed lines are the X-point locations. The neutral density at the separatrix does not vary substantially on the LFS, but there is a substantial increase as a function of increasing aspect ratio on the HFS. For the original MAST case, the neutral density from the HFS midplane up till the X-point is much lower. The largest increase is from aspect
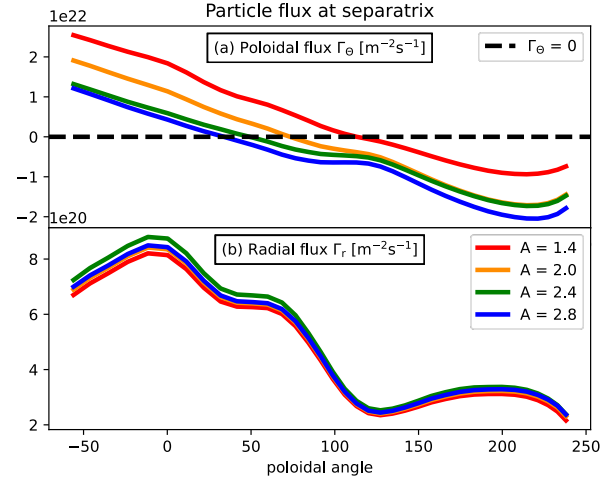
Particle flux at separatrix

Figure 7: Poloidal plot for poloidal and radial flux at the separatrix. The positive poloidal flux direction is toward the outer target and the positive radial flux direction is toward the wall. The black dashed line shows the poloidal flux stagnation point for each simulation case.

ratio 1.4 (red) to 2.0 (yellow), but the neutral density keeps increasing with increasing aspect ratio, see figure 6.

The increase with aspect ratio can be linked to an increase in parallel particle fluxes to the divertor. The continuity equation in B2.5 [4] is expressed as:

$$\frac{\partial n}{\partial t} + \frac{1}{\sqrt{g}}\frac{\partial}{\partial \theta}\left(\frac{\sqrt{g}}{h_\theta}\Gamma_\theta\right) + \frac{1}{\sqrt{g}}\frac{\partial}{\partial r}\left(\frac{\sqrt{g}}{h_r}\Gamma_r\right) = S_n \quad (2)$$

Where r stands for the radial and θ for the poloidal angle direction on the curvilinear B2.5 grid. In this equation n is the plasma density, S_n is the ionization source from the neutrals and $\Gamma_{r,\theta}$ is the radial and poloidal particle fluxes in the B2.5 grid. To map these particles fluxes from computation domain Cartesian grid to the 2D curvilinear grid, B2.5 uses geometry coefficients in radial, h_r, poloidal, h_θ, and toroidal h_ϕ direction. The coordinate transform Jacobian $\sqrt{g} = h_r h_\theta h_\phi$. Here $h_\phi = 2\pi R$, and $h_{r,\theta} = 1/\|\nabla r, \theta\|$ are identical for all our simulations at the separatrix.

The radial flux in the simulations shows no change as a function of the shift in R, see Figure 7 b), however the poloidal flux shifts 'downward' as a function of the increase in R. This means that as a function of aspect ratio, the flux increases towards the inner target and decreases towards the outer target. The second observation is that this means that the 'stagnation' point where the flow could go in either direction moves from the crown of the plasma for a MAST aspect ratio to the outer midplane as the aspect ratio increases. The change in poloidal flux is most pronounced in the initial increase in aspect ratio but saturates at the largest aspect ratios modeled in this paper.

This increase in parallel flux to the inner divertor means that more particles will be recycled in this region, as the recycling coefficient is fixed in these simulations. This means

the number of neutrals increases in the inner divertor as the simulations all reach a steady state with $\partial n/\partial t \sim 0$. The higher neutral density content in the inner divertor region shows up as an increase in neutral density at the separatrix close to the X-point on the high field side.

5. Discussion and Conclusion

In this paper, we investigate the role of aspect ratio on the opaqueness and the neutral density using SOLPS-ITER simulations. We shift the magnetic equilibrium and vessel in 4 simulations from 1.4 to 2.8 aspect ratio. Each simulation has the same transport coefficients and the same boundary conditions, which lead to similar plasma profiles. We find that the change in aspect ratio has no impact on the opaqueness of these plasma conditions. The opaqueness in these simulations are similar to previous results from DIII-D at low opaqueness on DIII-D [2]. Next steps would be to increase the opaqueness through an increase in the electron density and vary the temperature to alter the contributions of charge exchange to investigate whether aspect ratio in more fusion-relevant regimes would play a role.

The role of the aspect ratio on poloidal flows is not a result that can be tested experimentally. The stagnation point in normal aspect ratio tokamaks is on the LHF close to the midplane and depending on plasma conditions, drifts, and magnetic configuration either just above or below. As most spherical tokamaks are operated in a double null configuration, information on the stagnation point location and parallel flows specific to an ST is not applicable to this single lower null simulation. The next steps would include testing the impact of magnetic geometry and drifts on these results.

The impact of the increase in parallel flows to the inner divertor at normal aspect ratio and thus the creation of a higher neutral density region matches observations that a high neutral density front can form on the high field side in H-mode, as observed in both JET and AUG [14, 15]. The lack of a natural higher neutral density on the lower high field side in a spherical tokamak could also be responsible for why they might be more sensitive to localized fueling in altering density profiles and even access to H-mode [7].

To test this further, additional SOLPS-ITER modeling should be performed varying poloidal fueling locations and direct comparisons with new experiments which alter the poloidal fueling location and enhanced ionization measurements.

6. Acknowledgement

CRediT authorship contribution statement

Yi-Cheng Chuang: Methodology, Software, Analysis, Writing. **Saskia Mordijck:** Methodology, Idea, Supervision, Writing. **Richard Fitzpatrick:** Idea. **Richard Reksoatmodjo:** Software.

References

[1] Bonnin, X., Dekeyser, W., Pitts, R., Coster, D., Voskoboynikov, S., Wiesen, S., 2016. Presentation of the new solps-iter code package for tokamak plasma edge modelling. Plasma and Fusion Research 11, 1403102–1403102. doi:10.1585/pfr.11.1403102.

[2] Chaban, R., Mordijck, S., Rosenthal, A., Knolker, M., Laggner, F., Osborne, T., Schmitz, L., Thome, K., Wilks, T., 2024. The role of isotope mass on neutral fueling and density pedestal structure in the DIII-D tokamak. Nuclear Fusion 64, 046008.

[3] Costley, A., 2019. Towards a compact spherical tokamak fusion pilot plant. Philosophical Transactions of the Royal Society A 377, 20170439.

[4] Dekeyser, W., 2014. Optimal Plasma Edge Configurations for Next-Step Fusion Reactors. Ph.D. thesis. KU Leuven.

[5] Diallo, A., Canik, J., Göerler, T., Ku, S.H., Kramer, G., Osborne, T., Snyder, P., Smith, D., Guttenfelder, W., Bell, R., et al., 2013. Progress in characterization of the pedestal stability and turbulence during the edge-localized-mode cycle on national spherical torus experiment. Nuclear Fusion 53, 093026.

[6] Dunne, M.G., Potzel, S., Reimold, F., Wischmeier, M., Wolfrum, E., Frassinetti, L., Beurskens, M., Bilkova, P., Cavedon, M., Fischer, R., Kurzan, B., Laggner, F.M., McDermott, R.M., Tardini, G., Trier, E., Viezzer, E., Willensdorfer, M., Team, T.E.M., Team, T.A.U., 2016. The role of the density profile in the asdex-upgrade pedestal structure. Plasma Physics and Controlled Fusion 59, 014017. doi:10.1088/0741-3335/59/1/014017.

[7] Field, A., Carolan, P., Conway, N., Counsell, G., Cunningham, G., Helander, P., Meyer, H., Taylor, D., Tournianski, M., Walsh, M., et al., 2004. The influence of gas fuelling location on h-mode access in the mast spherical tokamak. Plasma physics and controlled fusion 46, 981.

[8] Hughes, J.W., LaBombard, B., Mossessian, D.A., Hubbard, A.E., Terry, J., Biewer, T., the Alcator C-Mod Team, 2006. Advances in measurement and modeling of the high-confinement-mode pedestal on the Alcator C-Mod tokamak). Physics of Plasmas 13, 056103.

[9] Kirk, A., Chapman, I., Harrison, J., Liu, Y., Nardon, E., Saarelma, S., Scannell, R., Thornton, A., et al., 2012. Effect of resonant magnetic perturbations with toroidal mode numbers of 4 and 6 on edge-localized modes in single null h-mode plasmas in mast. Plasma Physics and Controlled Fusion 55, 015006.

[10] Mordijck, S., 2020. Overview of density pedestal structure: role of fueling versus transport. Nuclear Fusion 60, 082006. doi:10.1088/1741-4326/ab8d04.

[11] Mordijck, S., Chaban, R., Reksoatmodjo, R., Balbin Arias, J., Chuang, Y.C., Loughran, J., Hughes, J., Rosenthal, A., Miller, M., Wilks, T., Laggner, F., Osborne, T., . Impact of ionization and transport on pedestal density structure in diii-d and alcator c-mod, IOP Publishing.

[12] Moser, A., Casali, L., Covele, B., Leonard, A., McLean, A., Shafer, M., Wang, H., Watkins, J., 2020. Separating divertor closure effects on divertor detachment and pedestal shape in diii-d. Physics of Plasmas 27.

[13] Parisi, J., Guttenfelder, W., Nelson, O., Gaur, R., Kleiner, A., Lampert, M., Avdeeva, G., Berkery, J.W., Clauser, C.F., Curie, M.T., et al., 2023. Kinetic-ballooning-limited pedestals in spherical tokamak plasmas. Nuclear Fusion .

[14] Potzel, S., Wischmeier, M., Bernert, M., Dux, R., Reimold, F., Scara-
bosio, A., Brezinsek, S., Clever, M., Huber, A., Meigs, A., et al.,
2015. Formation of the high density front in the inner far sol at asdex
upgrade and jet. Journal of Nuclear Materials 463, 541–545.

[15] Reimold, F., Wischmeier, M., Potzel, S., Guimarais, L., Reiter, D.,
Bernert, M., Dunne, M., Lunt, T., Team, A.U., et al., 2017. The high
field side high density region in solps-modeling of nitrogen-seeded h-
modes in asdex upgrade. Nuclear Materials and Energy 12, 193–199.

[16] Reksoatmodjo, R., Mordijck, S., Hughes, J., Lore, J., Bonnin, X.,
2021. The role of edge fueling in determining the pedestal density
in high neutral opacity alcator c-mod experiments. Nuclear Materials
and Energy 27, 100971. doi:https://doi.org/10.1016/j.nme.2021.
100971.

[17] Rosenthal, A., Hughes, J., Laggner, F., Odstrčil, T., Bortolon, A.,
Wilks, T., Sciortino, F., 2023. Inference of main ion particle transport
coefficients with experimentally constrained neutral ionization during
edge localized mode recovery on diii-d. Nuclear Fusion 63, 042002.

[18] Wilcox, R., Lore, J., . Solpsxport. URL: https://github.com/
ORNL-Fusion/SOLPSxport.

[19] Zohm, H., 2015. Magnetohydrodynamic stability of tokamaks. John
Wiley & Sons.